Cardiac Output Quantification Using Esophageal Photoplethysmography and Deep Learning

Author Name, *Member, IEEE*,
Another Author Name, *Fellow, OSA*

Abstract—This study presents a novel cardiac output quantification system that measures esophageal photoplethysmographic (PPG) signals, and obtains high measurement accuracy using deep learning-based method. To select the wavelength to improve predicting quality using the random forest model. The complete data set consised of 421 paired observations from the continue monitoring PPG and PiCCO datas in 7 pigs. The four-layer perceptron model is constructed based on 24 features extracted from PPG data and the corresponding cardiac outputs measured by PICCO. The system, evaluated with ten-fold cross-validation, demonstrated a high regression coefficient of 0.87, indicating high predictive accuracy. A Bland-Altman analysis confirmed the system's consistency, showing an output deviation of -0.079L/min and a percentage error (PE) of 0.0803.

Index Terms—Esophageal photoplethysmography, Deep learning, Cardiac output, Bland-Altman analysis.

1 Introduction

Cardiac output (CO) is the volume of blood the heart pumps per minute and is a crucial parameter for assessing cardiac pumping function and the state of systemic blood circulation [1]. The accurate measurement of CO is of significant importance for clinical diagnosis, evaluation of treatment effectiveness, and prognostic judgment. Changes in CO can reflect the functional state of the heart itself and the demands and adaptability of systemic circulation, which is vital for monitoring and managing clinical conditions such as heart failure and shock [2].

In recent years, non-invasive techniques for measuring cardiac output have been extensively studied. Photoplethysmography (PPG), in particular, has attracted attention due to its simplicity, low cost, and non-invasiveness [3]. The PPG signal reflects changes in blood volume within the vessels, allowing for the estimation of CO by analyzing the PPG waveform [4]. Advanced data analysis methods, such as deep learning, have been used to accurately extract CO from PPG signals, demonstrating the potential of this technology in clinical monitoring [5].

However, current studies indicate that the accuracy of traditional external PPG signals in extracting CO in specific situations, such as the perioperative period, is insufficient and significantly affected by various physiological and technical factors [6]. To overcome these limitations, researchers have begun exploring new PPG measurement sites and methods. Esophageal PPG measurement, as an emerging technology, promises to improve the accuracy and reliability of CO measurements due to the esophagus's proximity to the heart, which provides better signal quality than traditional surface PPG measurements.

In view of these challenges, this study proposes a novel deep learning perceptron model that analyzes 24 features extracted from esophageal PPG signals to continuously and minimally-invasively predict cardiac output. We collected PPG data and concurrent PiCCO measurements from 7 pig experiments. Since the measurement of cardiac output originates from PPG waveforms, only a single wavelength PPG waveform is needed. In order to select the PPG wavelength that can most accurately reflect cardiac output , we explored the quality of CO prediction by PPG waveforms at different wavelengths (940nm and 660nm) both in vivo and in vitro, finding that the 940nm wavelength PPG waveform provided the best quality of CO prediction. This finding offers important technical references for CO measurement using PPG signals.We then employed feature importance analysis to identify the most representative features and constructed a four-layer perceptron model. The model's performance was evaluated using ten-fold cross-validation, demonstrating close consistency with PiCCO measurements, as evidenced by a regression coefficient of 0.87. Furthermore, Bland-Altman analysis confirmed the model's high prediction accuracy with minimal bias and error.

2 Methods and Materials

2.1 Data

The physiological significance of cardiac output is the volume of blood pumped by the heart per minute. A 940 nm and 660 nm infrared light source was used to collect PPG waveforms. In measuring the cardiac output in animals, medical methods were used to control the cardiac output at different levels. Seven healthy pigs were used as experimental subjects for measuring the PPG signal and cardiac output. After anesthetizing the experimental subjects, surgery was performed to open the thoracic cavity, and each time 50 ml of continuous proportional diluted blood was induced to decrease the cardiac output. Subsequently, each time 50 ml of continuous blood transfusion was induced to increase the cardiac output of the experimental pigs. After each dilution of blood or transfusion, the cardiac output was measured as

standard using a PICCO monitor. During the experiment, a 940 nm infrared reflection sensor was aligned and placed inside the thoracic cavity alongside the descending aorta, and the PPG signal was collected by a front-end PPG signal sensor and Texas Instruments (TI) AFE4400 chip for calculating the cardiac output about two to four minutes after each perfusion or dilution of the experimental subject's blood. By collecting PPG signals from seven experimental pigs and corresponding time period cardiac output measurements by the PICCO standard, seven experimental data sets were obtained, comprising 389 experimental data cases, each containing about 120,000 in-body PPG signal points with a sampling rate of 500 Hz and a wavelength of 940 nm and 660nm, as well as the corresponding period's cardiac output measured by the PICCO detector. The experiment complied with national regulations on experimental animal welfare and ethics, obtaining ethical approval number 2019056A.

2.2 Pre-Preprocessing

2.2.1 PPG Feature Extraction Process

For the raw PPG data packets, experimental subjects may exhibit jitter during the PPG data measurement, and the waveform data contains a large amount of noise that needs filtering. Due to the effects of sensor placement and ambient light contamination, there are segments of PPG waveforms with poor quality. A waveform auto-correlation algorithm is used to select good segments of PPG waveforms for feature extraction.

PPG waveforms contain a wealth of information on individual cardiac and vascular functions. The normal PPG waveform cycle reflects the heart rate, and the cycle variability reflects the heart rate variability; components below 0.5 Hz reflect the respiratory component, but due to the use of ventilators for oxygen supply to experimental subjects in experiments, the PPG signals of experimental subjects cannot effectively reflect the low-frequency respiratory component, and this feature is discarded; the presence of the dicrotic notch value in PPG waveforms reflects the function of cardiac valve closure, indirectly reflecting the health level of the heart; parameters of the area under the PPG waveform, such as the area under the rising edge reflecting cardiac pumping ability, the area before the dicrotic notch value reflecting the pumping function during the ejection phase of the heart, and the total area under the curve reflecting the blood volume flowing through the heart; calculating pulse wave dynamics parameters from PPG waveforms can reflect whether the cardiac pumping function is strong; long-term and short-term heart rate variability calculated from PPG waveforms reflect the heart's responsiveness to autonomic nervous system (ANS) regulation.

$$CO = HR \times SV \tag{1}$$

where CO is the cardiac output, HR is the heart rate, and SV is the stroke volume. This formula is highly correlated with the heart rate, the volume of blood ejected during the cardiac ejection phase, and the health level of the heart. Using PPG signals, features such as average heartbeat interval, heartbeat period variability, and others serve as feature variables, with the corresponding period's cardiac output as the prediction variable, constructing a four-layer perceptron model to accurately predict cardiac output. The extraction of physiological features from PPG signals is shown in Figure 1.

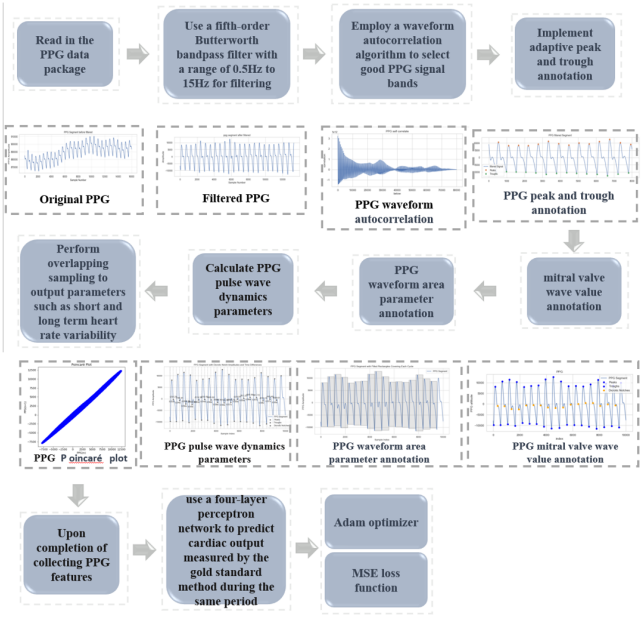

Fig. 1. Extraction of physiological features from PPG signals.

First, read in the PPG data packets and apply a fifth-order Butterworth band-pass filter to the raw PPG data, with a passband from 0.5 Hz to 15 Hz. Perform autocorrelation analysis on the PPG waveform to select good-quality PPG segments. Use an adaptive peak-to-valley annotation algorithm to mark the peak and valley values of the PPG waveform, and an adaptive mitral wave value annotation algorithm to mark the mitral wave values of the PPG waveform. Calculate the area parameters of the PPG waveform and the pulse wave dynamics parameters. Then, use overlapping sampling to draw the Poincaré plots for long-term and short-term PPG waveforms, outputting the area parameters of the Poincaré plots as well as the long-term and short-term heart rate variability. This completes the extraction of 24 features from the PPG waveform.

2.2.2 Adaptive Peak and Valley Annotation of PPG Waveforms

The peak and valley values of a PPG waveform are used to define a waveform cycle, outputting heart rate and heart rate variability parameters. However, due to noise during the sampling process, some PPG waveforms may exhibit local dips or spikes, which can be mistakenly identified as peak or valley values by the `findpeaks` function in the Python's pandas library. To correctly annotate the peak and valley values of a PPG waveform, it is necessary to pass a minimum number of samples between peaks as the `distance` parameter to the `findpeaks` function. By using Fast Fourier Transform to draw the PPG waveform spectrum, the main peak value of the spectrum represents the average heart rate frequency. At a sampling rate of

500Hz, the average number of points between peaks of the PPG signal is given by Equation :

$$\text{Average number of points} = \frac{500}{f_{\text{average heart rate frequency}}} \quad (2)$$

Considering the changes in heart rate with physiological rhythms, the `distance` parameter is set according to Equation:

$$\text{Distance parameter} = \frac{500}{f_{\text{average heart rate frequency}}} - 50 \quad (3)$$

As shown in Figure 2, the peaks and valleys of the filtered PPG signal are annotated.

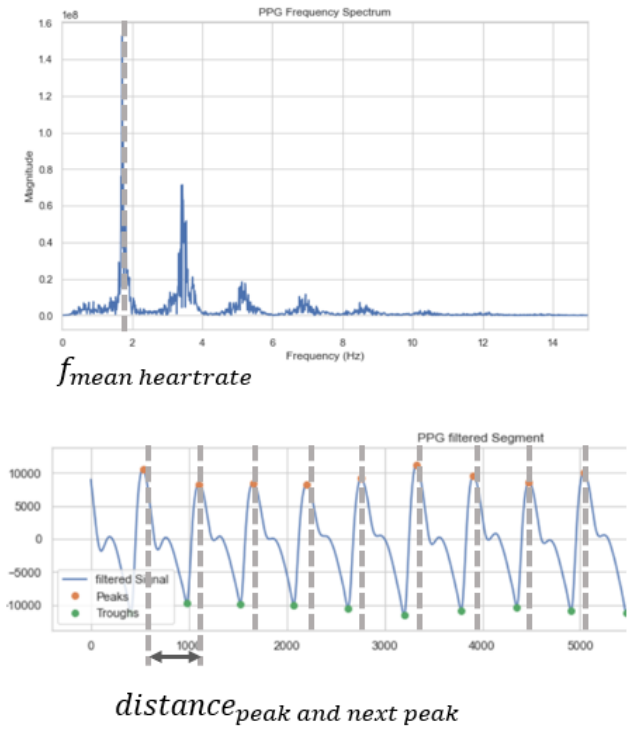

Fig. 2. Annotation of peaks and valleys in the filtered PPG signal.

2.2.3 Adaptive Annotation of Mitral Valve Waves

The mitral valve, an important valve between the left atrium and left ventricle, plays a crucial role during the cardiac diastolic phase. During this phase, the backflow of blood impacts the mitral valve, creating a small dip between the peak and the second valley within a cycle on the PPG waveform. The mitral wave value is vital for assessing the health level of cardiac valves, calculating pulse wave dynamics parameters, and determining the volume parameters of the cardiac ejection phase. The presence of local noise in collected PPG signals makes the annotation of mitral wave values challenging. To accurately annotate the mitral wave values, an adaptive mitral wave value annotation algorithm is employed. The algorithm process is as follows: For PPG signals with annotated peaks and valleys after filtering, use adjacent valley values to define a cycle. Within this cycle, search for a point between the peak value and the second valley where the first derivative is zero, and the second derivative is minimal. Set a condition that the position of this point must have a perpendicular distance from the peak and valley greater than 0.2 times the vertical distance between the peak and the second valley within the cycle, to prevent incorrectly marking noise dips or spikes near peaks and valleys as mitral wave value points. Also, calculate the ratio of the horizontal distance from the mitral wave value to the first valley and the horizontal distance between the first and second valleys within a PPG cycle. Based on physiological theory, for the same individual, the position of the mitral wave value in a cycle of the PPG signal is relatively constant. Using a 0.95 confidence T-test, obtain the mean ratio value for all PPG signals where the mitral wave value can be annotated. Then, use the mean ratio value to annotate mitral wave value points in PPG cycle signals where the mitral wave value is not clearly visible, as shown in Figure 3, completing the adaptive annotation of the mitral valve wave.

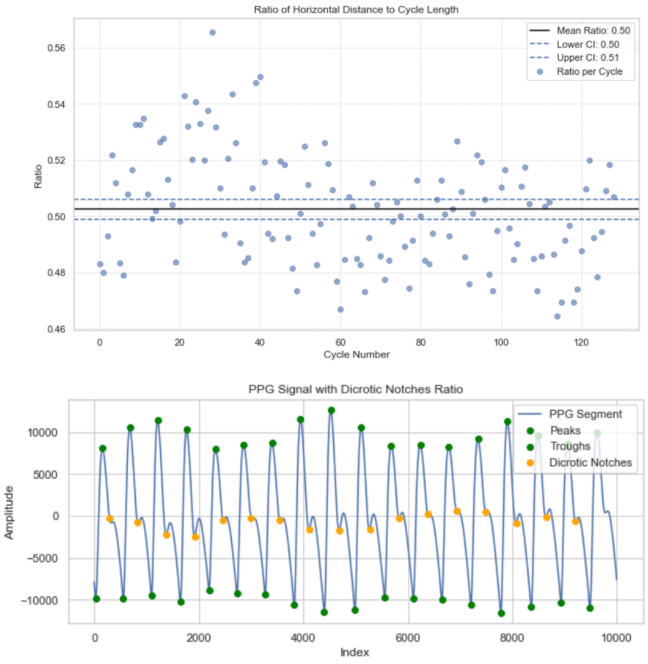

Fig. 3. Adaptive annotation of the mitral valve wave in a PPG waveform.

2.2.4 PPG Waveform Area Parameters and Pulse Wave Dynamics Parameters Extraction

As shown in Figure 4, within one cycle of the PPG waveform, the AC component A_1, DC component A_2, dicrotic notch component A_3, and the total area within a rectangular frame for one cycle of the PPG waveform $S_1 + S_2 + S_3 + S_4$, the rising limb area S_2, the ejection period area $S_2 + S_3$, and the total area under the curve within one cycle of the PPG waveform $S_2 + S_3 + S_4$ are marked.

The PPG signal contains DC and AC components. When the cardiac output increases, the logarithmic value of the DC component can reflect its higher-order terms and is related to the cardiac output:

$$\text{PPG}_{\ln \text{DC ratio}} = \ln(\overline{A_2}) \quad (4)$$

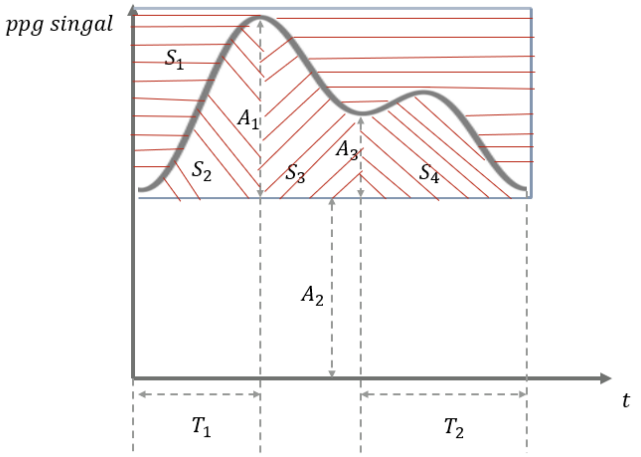

Fig. 4. PPG Waveform Area Parameters and Pulse Wave Dynamics Parameters.

Ratios of the AC component and the dicrotic notch component to the DC component:

$$\text{PPG}_{\text{AC to DC ratio}} = \frac{A_1}{A_2} \tag{5}$$

$$\text{PPG}_{\text{dicrotic notch to DC ratio}} = \frac{A_3}{A_2} \tag{6}$$

Define area parameters R_1, R_2, R_3, R_4:

$$R_1 = \frac{S_2 + S_3 + S_4}{S_1 + S_2 + S_3 + S_4} \tag{7}$$

$$R_2 = \frac{S_2}{S_1 + S_2 + S_3 + S_4} \tag{8}$$

$$R_3 = \frac{S_2 + S_3}{S_1 + S_2 + S_3 + S_4} \tag{9}$$

$$R_4 = \frac{S_2 + S_3}{S_4} \tag{10}$$

Existing research shows that the PPG waveform and arterial waveform together predict cardiac output with high reliability, defining a pulse wave dynamics strength parameter:

$$\text{PPG}_{\text{dynamics parameter}} = \frac{A_1}{T_1} + \frac{A_3}{T_2} \tag{11}$$

2.2.5 Extraction of Heart Rate and Heart Rate Variability Parameters from PPG Signal

Extraction of parameters such as heart rate and heart rate variability from PPG signals reflects the heart's adaptability to physiological demands. These parameters have a strong correlation with cardiac output on a physiological level. Parameters extracted from the PPG signal include:

Heart Rate (bpm): Represents the number of heartbeats per minute, calculated by measuring the time interval between adjacent peaks in the PPG signal. The calculation formula is:

$$\text{HR} = \frac{60,000}{\text{IBI (ms)}} \tag{12}$$

Inter-Beat Interval (IBI): The time difference between consecutive heartbeat peaks.

Standard Deviation of NN intervals (SDNN): Reflects the overall variability of all normal-to-normal (NN) intervals.

$$\text{SDNN} = \sqrt{\frac{1}{N-1}\sum_{i=1}^{N}(NN_i - \overline{NN})^2} \tag{13}$$

Standard Deviation of Successive Differences (SDSD): Reflects the variability of consecutive heartbeat intervals.

$$\text{SDSD} = \sqrt{\frac{1}{N-1}\sum_{i=1}^{N-1}(NN_{i+1} - NN_i)^2} \tag{14}$$

Root Mean Square of Successive Differences (RMSSD): Reflects the square root of the mean of the squares of successive differences between normal heartbeats.

$$\text{RMSSD} = \sqrt{\frac{1}{N-1}\sum_{i=1}^{N-1}(NN_{i+1} - NN_i)^2} \tag{15}$$

NN50 count (pNN50): The percentage of the number of interval differences of successive NN intervals that are greater than 50 ms.

$$\text{pNN50} = \frac{\text{Number of NN50}}{N-1} \times 100\% \tag{16}$$

Heart Rate Median Absolute Deviation (HR_MAD): Reflects the stability of the median heart rate.

$$\text{HR\_MAD} = \text{med}(|NN_i - \text{med}(NN)|) \tag{17}$$

The Poincaré plot provides a two-dimensional visual representation of HRV by plotting each NN interval against the next, allowing observation of heart rate dynamics' complexity and variability. The shape of the Poincaré plot can be described by two orthogonal standard deviations, SD1 and SD2, reflecting short-term and long-term variability, respectively.

$$\text{SD1} = \sqrt{\frac{\text{SDSD}^2}{2}} \tag{18}$$

$$\text{SD2} = \sqrt{2 \times \text{SDNN}^2 - \frac{\text{SDSD}^2}{2}} \tag{19}$$

The area of the ellipse formed by SD1 and SD2 on the Poincaré plot, reflecting the overall HRV, is given by:

$$\text{S} = \pi \times \text{SD1} \times \text{SD2} \tag{20}$$

The SD1/SD2 Ratio reflects the balance of the autonomic nervous system:

$$\text{SD1/SD2} = \frac{\text{SD1}}{\text{SD2}} \tag{21}$$

2.2.6 Data Statistics

After the extraction of 24 numerical features from PPG signals, Table 1 displays the statistical information for some of these features. The kernel density distribution curve of the cardiac output measured by PICCO in experimental subjects is illustrated in Figure 5.

TABLE 1
Statistical Information of Selected PPG Signal Features

Metric	Mean	Variance	Std Dev	CV
Average Heartbeat Interval	99.9	410.72	20.27	0.2
Heartbeat Period Variability	625.16	15 797	125.69	0.2
AC/DC Component Ratio	0.07	0	0.07	1.05
Dicrotic Notch to DC Ratio	0.04	0	0.06	1.35
ln Average DC Component	11.26	1.6	1.27	0.11
Amplitude Variation Period	1.73	7.35	2.71	1.56
R1	0.47	0.01	0.08	0.17
R2	4.85	5.45	2.33	0.48
R3	0.31	0	0.06	0.2
R4	0.37	0.01	0.08	0.21
CO	3.67	0.83	0.91	0.25

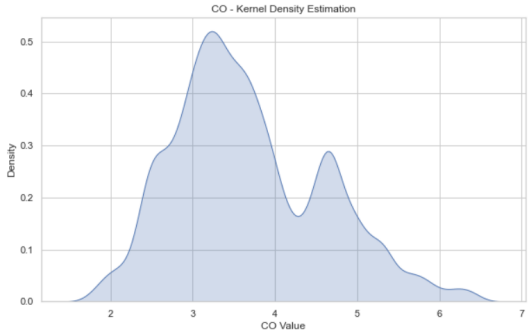

Fig. 5. Kernel Density Distribution Curve of Cardiac Output Measured by PICCO

2.3 Proposed Model

We utilized 24 features extracted from PPG signals as feature variables, with the cardiac output detected by the PICCO monitor during the corresponding period serving as the predictive variable (label), all subjected to min-max normalization. Figure 6 illustrates the feature importance graph of feature variables to the predictive variable. It is evident that the heart rate, heart rate variability, and the ejection period extracted from the PPG waveform make significant contributions to predicting cardiac output.

A four-layer perceptron deep learning network was constructed to process a 24-dimensional input vector. The input vector undergoes transformation through the first hidden layer, followed by batch normalization and activation via the ReLU (Rectified Linear Unit) function, resulting in a 64-dimensional vector. This vector is then passed through a second hidden layer, where it is again batch normalized and activated with the ReLU function, reducing its dimensionality to 32. Following a similar procedure, the third hidden layer further processes the vector, applying batch normalization and ReLU activation to produce a 16-dimensional vector. Finally, the output layer performs a linear transformation

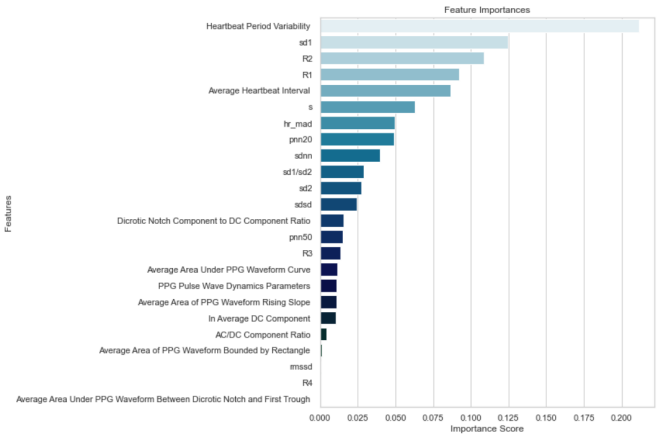

Fig. 6. Feature importance of the predictive variable.

to produce a one-dimensional output, which represents the predicted heart output value. During the network's back-propagation process, the ADAM optimizer and the MSE (Mean Squared Error) loss function are employed.The MSE loss function, used for regression problems, measures the average squared difference between the estimated values and the actual value. Mathematically, it is defined as:

$$MSE = \frac{1}{n}\sum_{i=1}^{n}(Y_i - \hat{Y}_i)^2 \tag{22}$$

where n is the number of observations, Y_i is the actual value, and $\hat{Y}_i$ is the predicted value.

The structure of the deep learning network is illustrated in Figure 7.

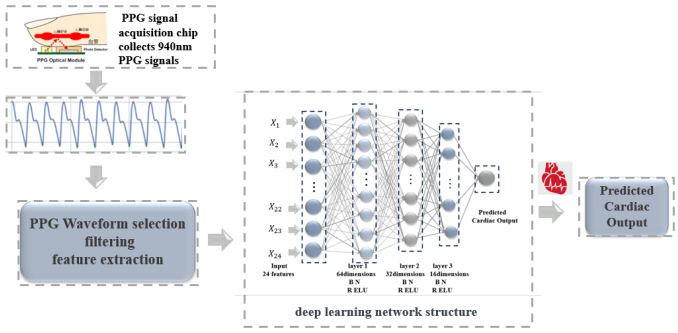

Fig. 7. The structure of the deep learning network.

2.4 Training the Deep Learning Network

The dataset was subjected to ten-fold cross-validation, where the original dataset was randomly divided into ten equal subsets. In each round, a process of ten training and validation sessions was conducted, utilizing nine subsets for training and one subset for testing, to calculate the Mean Squared Error (MSE) loss function on the test set. The training was carried out for 20,000 iterations. During the training process, the MSE loss function graph for the test set was plotted, as shown in Figure 8.After 20,000 rounds of training, the the normalized cardiac output loss function value on the test set reached 0.002084L/min.

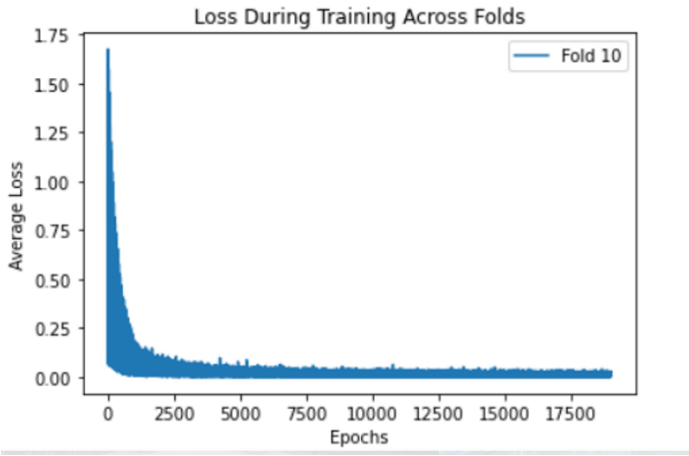

Fig. 8. The Mean Squared Error loss function graph for the test set.

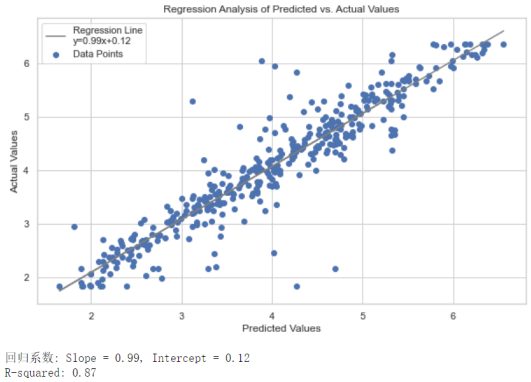

Fig. 9. Regression fit between predicted cardiac output values and PICCO-measured values.

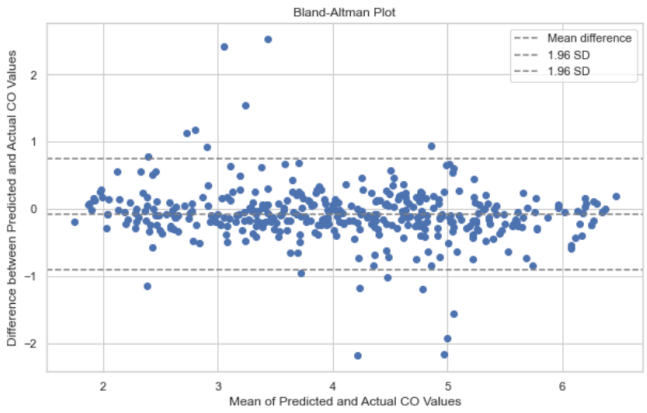

Fig. 10. Bland-Altman plot showing the concordance between model predictions and PICCO measurements.

3 Results

After the training of the deep learning model was completed, the weight parameters were saved. The model's output of predicted cardiac output values on the test set was regressed against the cardiac output values measured by the PICCO monitoring device, as shown in Figure 9, achieving a regression coefficient R^2 of 0.87. To further investigate the correlation between model-predicted cardiac output values and those measured by the PICCO device, a Bland-Altman plot was drawn as illustrated in Figure 10. The two measurements showed a strong concordance relationship, with approximately 93.9% of the model output prediction values falling within the limits of agreement. As shown in Table 2, the percentage error obtained was -8.03%, which is within the clinically acceptable percentage error range of 30%.

To further study the accuracy of predicting cardiac output using different wavelengths and intracorporeal versus extracorporeal PPG signals, a single animal experiment involving 51 experimental cases was conducted. In the experiment, PPG signals were measured on the pigs using wavelengths of 660nm and 940nm, both inside the thoracic cavity and on the tail. Twenty-four features of the PPG signals were extracted in the same manner as feature variables, with the cardiac output detected by the PICCO during the corresponding period as the prediction variable. Given the small size of the dataset, which was not suitable for a deep learning network, a random forest prediction model was selected. The dataset underwent ten-fold cross-validation, and regression analysis and Bland-Altman plot consistency checks of the model's output of predicted cardiac output against the PICCO-measured cardiac output were performed as shown in Table 3. The regression coefficient R^2 for the 940nm intracorporeal signal reached 0.79, with approximately 96.5% of the model output prediction values falling within the limits of agreement, significantly surpassing the predictive ability of the 660nm intracorporeal waveform and the 940nm extracorporeal waveform for cardiac output.

4 Discussion

This study was based on the extraction of 24 features from the 940nm intrabody PPG signals of experimental pigs to predict cardiac output values, showing good predictive performance on the test set. Given the physiological structural similarities between pigs and humans, we also applied the model with a built-up collection system to collect PPG signals from experimental volunteers, recording the predicted cardiac output values of subjects in different states, demonstrating the physiological rationale and sensitivity of the model for clinical patients. The experimental data is shown in Table 4:

TABLE 2
Predicted CO And PICCO Statistical Analysis Summary

Measurement	Value
Bias (L/min)	-0.079
STD (L/min)	0.420
95% LOA (L/min)	-0.902 to 0.743
MAE (L/min)	0.273
MSE (L/min)	0.182
RMSE (L/min)	0.427
95% Confidence Interval of Difference	(-0.121, -0.038)
R (Correlation Coefficient)	0.934
PE (Percentage Error)	8.03%

TABLE 3
Comparison of PPG measurements inside and outside at different wavelengths.

	940nmPPGinside	660nmPPGinside	940nmPPGoutside
R-squared	0.79	0.72	0.6
PEI*	96.5%	91.1%	82.0%

* PEI represents Percentage of estimates within consistency limit.

TABLE 4
Experimental Data

Subject's Age	Gender	Experiment Posture	Experiment State	Predicted CO
48	Female	Sitting	Calm	3.7L/min
48	Female	Lying	Calm	4.1L/min
22	Male	Sitting	Calm	3.5L/min
22	Male	Sitting	Excited	3.7L/min
46	Male	Sitting	Excited	3.4L/min

5 Conclusion

This paper proposes a non-invasive algorithm to accurately predict cardiac output based on PPG signals in animal experiments. The regression coefficients and percentage error (PE) of the algorithm meet clinical standards, and it has the ability to generalize the prediction of human cardiac output. At the same time, by analyzing the accuracy of cardiac output prediction of different wavelengths and intrabody versus extrabody PPG signals, it was found that the 940nm intrabody PPG signal has the best accuracy in predicting cardiac output.

6 Acknowledgments

Thanks to the support of the National Natural Science Foundation of China, to Professor Gao Bo from the School of Physics at Sichuan University for his careful guidance, to West China School of Medicine for providing experimental data, and to the research team members for their hard work and study.

References

[1] DA Reuter and AE Goetz. Measurement of cardiac output. *Anaesthesist*, 54(11):1135–1151, 2005.

[2] L Mathews and RK Singh. Cardiac output monitoring. *Ann Card Anaesth*, 11(1):56–68, 2008.

[3] X García, L Mateu, J Maynar, J Mercadal, A Ochagavía, and A Ferrandiz. Estimating cardiac output: Utility in clinical practice. available invasive and non-invasive monitoring. *Med Intensiva*, 35(9):552–561, 2011.

[4] DB Northridge, IN Findlay, J Wilson, E Henderson, and HJ Dargie. Non-invasive determination of cardiac output by doppler echocardiography and electrical bioimpedance. *Br Heart J*, 63(2):93–97, 1990.

[5] J Penttilä, A Snapir, E Kentala, J Koskenvuo, J Posti, M Scheinin, H Scheinin, and T Kuusela. Estimation of cardiac output in a pharmacological trial using a simple method based on arterial blood pressure signal waveform: a comparison with pulmonary thermodilution and echocardiographic methods. *Eur J Clin Pharmacol*, 62(6):401–407, 2006.

[6] S Hagl and CF Vahl. Intraoperative diagnosis–measuring heart time volume and assessment of shunts. *Z Kardiol*, 79:Suppl 4:107–117, 1990.